Effect of Deformation Mode of Cylindrical Tubes with Corrugated Surface Dimensional Errors

Shigeyuki Haruyama[1], Daiheng Chen[2], Ken Kaminishi[1], Takuya Niyama[3]
1 Management of Technology, Yamaguchi University, 2-16-1 Tokiwadai, Ube-shi, Yamaguchi, Japan
2 Department of Engineering, Tokyo University of Science, 1-3 Kagurazaka, Shinjuku-ku, Tokyo, 162-8601 Japan
3 Department of Science and engineering, Yamaguchi University, 2-16-1 Tokiwadai, Ube-shi, Yamaguchi, Japan
(E-mail: p038ve@yamaguchi-u.ac.jp; haruyama@yamaguchi-u.ac.jp)

Abstract: A cylindrical tube with a corrugated surface in the axial direction has excellent energy absorption characteristics as an automobile impact-absorbing part. In this paper, the difference in the deformation mode between the analysis results using a finite element method (FEM) and the experimental results obtained using actual cylindrical tubes is investigated. It is shown that the difference is caused by initial irregularities such as size errors. Furthermore, it can be denoted that the load–displacement curve and the deformation diagram are good agreement in the S-mode. However, there is a difference in the deformation diagram and a slight shift in the load–displacement curve in the P-mode.
Key words: Plasticity; Finite Element Method; Numerical Analysis; Deformation; Characteristics

1 Introduction

A tubular aluminum alloy is widely used for making automobile body structures in order to make cars relatively light and improve car safety during vehicle collisions. Recently, corrugated surface materials in the axial direction have been noted to improve the impact energy absorption characteristics of thin-walled tubular structures [(1)-(9)]. A virtual Material follow a bilinear hardening rule using the large elastoplastic deformation numerical analysis by Finite Element Method [(6)], investigation effect of hardening of the material and geometry for energy absorption characteristics of cylindrical tubes with corrugated surface. The deformation of cylindrical tubes depends on the geometry of the corrugated cylindrical tubes with respect to the corrugated surface can be classified into mode ignore corrugation and mode deformation axi-symmetric, corresponding to corrugated as the S-mode and P-mode. The load efficiency is expressed by the ratio of the average compressive stress and the maximum compressive stress and has the maximum value near the boundary of the S-mode and the P-mode. Chen et al. have not investigated dimensional errors that occur when a real part is used as the energy absorbing part because the large elastoplastic deformation numerical analysis with Finite Element Method using virtual material. It is necessary to examine in detail the challenges of using actual thin-walled cylindrical tubes with a corrugated surface. In this paper, the effects of the dimensional error of the shape of the deformation material are characterized and the effect on the mode distribution of the real materials is estimated using a numerical analysis of a large elastoplastic deformation by a finite element method using the material properties of the real part. A quasi-static compression experiment of cylindrical tubes with a corrugated surface fabricated by cutting the aluminum alloy that is used as an energy absorbing member is carried out.

2 Analytical and Experimental Methods

2.1 Specimens

The specimens are made from a solid extrusion rod aluminum alloy (A5052) (φ 80 [mm], length 4000 [mm]), which is used for automotive structural components. The mechanical properties of specimens are determined using the JIS4 specimen with tensile testing. Tensile testing is performed using a Shimadzu Autograph (AG-10T) testing machine with a displacement meter (video-type non-contact extensometer DVE-200S). The load–displacement is measured at a sampling rate of 100 Hz by a memory recorder analyzer (Kyowa Electronic Instruments EDX-1500A), and the obtained stress-nominal strain curve is shown in Fig.1.

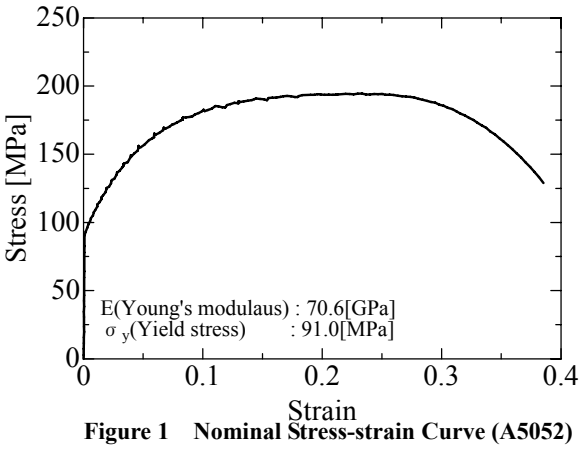

Figure 1 Nominal Stress-strain Curve (A5052)

2.2 Numerical analysis experiment

The commercial FEM analysis package MSC. Marc is used in this study to analyze the large elastoplastic deformations as the axial crushing deformations (Fig.2). The initial tube lengths of the corrugation are set to L = 105 mm and the radius is set to R = 27.5 mm. The effects of various geometric parameters are as follows: wall thickness t, corrugation wavelength 2λ, and amplitude a. The tubes are modeled using four-node three-dimensional quadrilateral thickness shell elements and four-node axi-symmetric isoparametric quadrilateral elements. The size of the elements is estimated by dividing one wavelength in the axial direction into 8–16 sub lengths, and the shell elements are divided in the circumferential direction to obtain the approximately square elements. The solid elements are also divided in the thickness direction to obtain the approximately square elements. The material properties are determined using the mechanical properties shown in Fig.1.

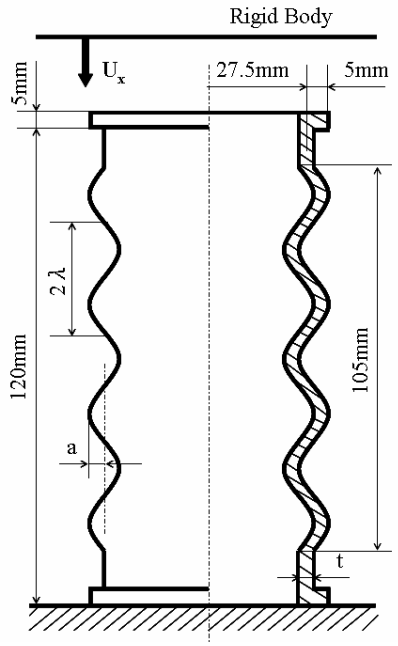

Figure 2 Tube Geometry and Loading Condition

Table 1 Shape of Analysis Model

t [mm]	2λ [mm]	a [mm]
2.0	16.2, 19.1, 23.3, 30.0	1.0, 2.0, 3.0
3.0	16.2, 19.1, 23.3, 30.0	1.0, 2.0, 3.0
5.0	16.2, 19.1, 23.3, 30.0, 42.0	1.0, 2.0, 3.0

Boundary conditions: The bases of the tubes are completely fixed at a rigid floor, and the axial compression is imposed from above by modeling a rigid body moving downward according to the displacement control. The contact condition between the upper tubes and the rigid body is determined using the Glue functionality, which is completely fixed upon contact with the upper tube and body. Furthermore, in the numerical calculation, von Mises yield conditions are used for following the plastic yield conditions. The updated Lagrangian method is used for formulating the geometric nonlinear

behavior, and the algorithm is based on the Newton–Raphson method used to solve the nonlinear equations. The deformation mode of a cylindrical tube with a corrugated surface is also found from the Chens[5] study such that the mode can further be classified into "corresponding to corrugation modes" and "non-corresponding to corrugation modes, called N-mode here." Moreover, the corresponding to corrugation mode can be classified into two different patterns: in one pattern, folds occur along the corrugations in the axial direction and are axially symmetric, called the symmetric mode here, and in the other pattern, the folds does not match the corrugations, called the non-symmetric mode here. Furthermore, the symmetric mode can be classified into "Progressive" and "Simultaneous" modes (hereafter, we refer P- and S-modes, respectively). However, the decision near the boundary of the deformation mode is difficult because there is a non-clear standard for reaching the mode decision between the P- and S-modes. Previous studies: However, the non-dimensional load incline may be slightly minus. Therefore, in this research, apart from the monotonous increase in load, even if the load slope becomes negative, the prediction method assumed to be S-mode will be used if the wave rates of the average load at the range between the load declination position and the position of another load increase are within -5%.

Further, thus far, the studies that have been conducted have mainly focused on the P-mode and the S-mode range, which is considered to be an efficient energy absorbing component. Therefore, in this study, an analysis of a model of cylindrical tubes with a corrugated surface of the combined shape with thickness t, wavelength 2λ and amplitude a as shown in Table1 is conducted.

2.3 Substance evaluation experiment

There are many processing methods of cylindrical tubes and different dimensional accuracies; however, the specimen of this research is made with NC Lathe. The specimen has the same shape (Fig.2) as that used in the FEM analysis. Both ends of the flange prevent the inclination of fixing a specimen or enters the upper and lower ends. The dimensions of the specimen are shown in Table 2, and the typical examples of the appearance of the specimen are shown in Fig.3. The experimental device of axial crushing has a laser displacement sensor made of SUNX (HL-C135CBK10) installed in the 200t Universal Testing Machine made by Shimadzu; the load and the displacement are recorded by the memory recorder analyzer (Kyowa Electronic Instruments EDX-1500A) at a sampling rate of 100 Hz. Then, the load–displacement curve is plotted. The deformation of the specimen is synchronous with the measurement of the memory recorder analyzer using a digital video camera (frame rate: 30 fps). A specimen is installed in a manned that there is no forced fixation on the upper and lower surfaces; a lubricant is applied to increase the degree of adhesion at both the ends. The load–displacement curve and the S-mode deformation diagram agree well. However, in the P-mode, the load–displacement curve has a slight shift and the deformation diagram illustrates the difference. The P-mode varies widely because of the local deformation of the folds' wavelength, and the S-mode is stable because of the increase in the load during deformation.

Table2 Specimen Shape

t [mm]	2λ [mm]	a [mm]
2.0	19.1 23.3 30.0	1.0, 2.0, 3.0 2.0, 3.0 2.0
3.0	19.1 23.3 30.0	1.0, 2.0, 3.0 1.0, 2.0, 3.0 2.0
5.0	19.1 23.3 30.0	2.0 2.0 2.0

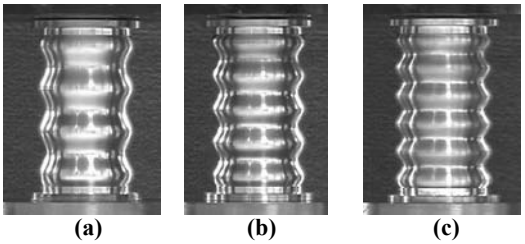

(a) (b) (c)

Figure 3 Specimens (a) 2λ = 30.0 [mm], a = 3.0 [mm], t = 2.0 [mm] (b) 2λ = 23.3 [mm], a = 3.0 [mm], t = 2.0 [mm] (c) 2λ = 19.1 [mm], a = 2.0 [mm], t = 5.0 [mm]

3 Result

3.1 Analytical and experiment result

Fig.4 shows the results of the plotted deformation mode of analysis and the actual evaluation experiment with amplitude a, horizontal axis and wavelength 2λ, and vertical axis for each thickness t. The trend of the distribution modes in both the analysis and the actual evaluation experiment favors the S-mode when the amplitude a is small and the wavelength 2λ is large. Figs.5 and 6 show the load–displacement curve and deformation at $t = 5.0$ *mm,* $2\lambda = 19.1$ *mm,* and $a = 2.0$ *mm*, both the actual

evaluation experiments and analysis are in the S-mode. Figs.7 and 8 (*t = 2.0 mm, 2λ = 30.0 mm, a = 3.0 mm*) illustrate the results obtained in the P-mode. It is found that the load–displacement curve and the deformation diagram are in good agreement in the S-mode; however, there is a difference in the deformation diagram and a slight shift in the load–displacement curve in the P-mode. The P-mode has relatively large variability because there is a local variant of the folds' wavelength. Further, the S-mode is stable because it increases the load during deformation. Moreover, the appearance of the specimen with *t = 2.0 mm, 2λ= 30.0 mm, a = 2.0 mm, and t = 2.0 mm, 2λ = 19.1 mm, a = 1.0 mm* corresponded to the corrugation modes in the analysis and the non-symmetric mode in the experiment, and may differ between the analysis and the experiment as the S-mode in the analysis and the P-mode in the experiments. Next, we investigate the geometry, *t = 2.0 mm, 2λ = 30.0 mm, a = 2.0 mm*, and *t = 2.0 mm, 2λ = 19.1 mm, a = 1.0 mm*, of the P-mode in the analysis and of the non-symmetric-mode in the experiment. The fold wavelength $2\lambda_0$ determined by the analysis during the collapse of the cylindrical tube is $2\lambda_0$*=25.2mm*. Therefore, *2λ = 23.3 mm* is almost equal $2\lambda_0$; however, at *2λ = 19.1 mm,* $2\lambda < 2\lambda_0$, and at *2λ = 30.0 mm,* $2\lambda > 2\lambda_0$.

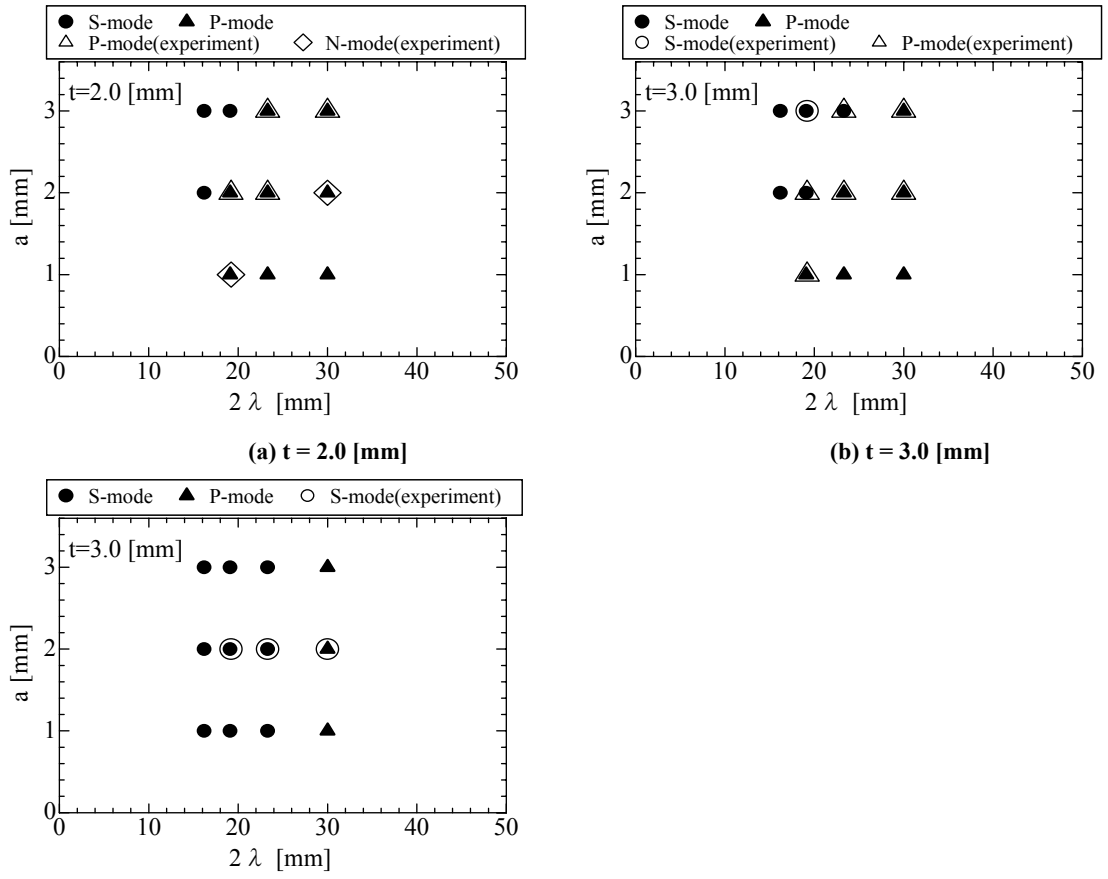

(a) t = 2.0 [mm]

(b) t = 3.0 [mm]

(c) t = 5.0 [mm]

Figure 4 Mode Classification Chart from FEM and Experiment: (a) t = 2.0[mm], (b) t = 3.0[mm], (c) t = 5.0[mm]

Furthermore, the deformation tends to be non-axi-symmetric when the thickness *t* is relatively small and the wavelength of wave *2λ* is equal to the fold wavelength produced during the axial crushing of cylindrical tubes, $2\lambda_0$, as mentioned by Chen[6]. Further, when it moves away from the easily axi-symmetrically deformed $2\lambda_0$, a deformation that does not follow the wave occurs easily. Thus, the deformation mode assumed as the P-mode in the analysis that contains some external disturbance from the experiment will be considered to be the non-symmetric-mode.

Furthermore, in the experiments and analysis using FEM, there was no deformation of the S-mode from the P-mode and of the P-mode from the non-symmetric-mode.

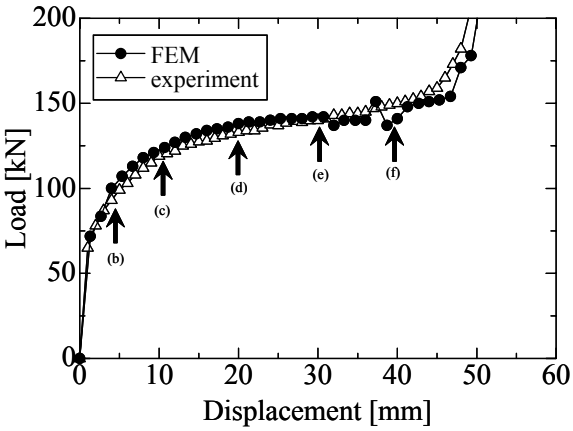

Figure 5 Load-deflection curve of tube with t = 5.0 mm, a = 2.0 mm, 2λ = 19.1 mm

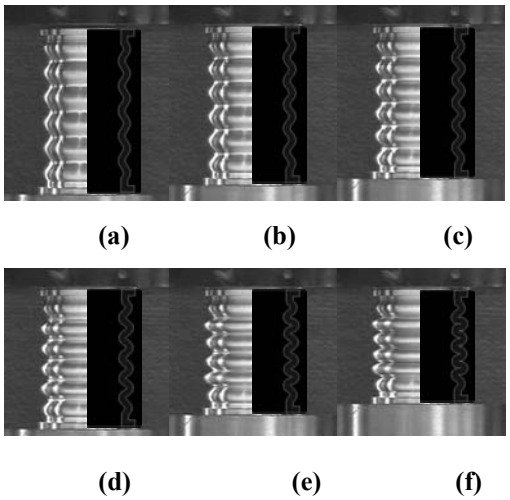

Figure 6 Transformation figures of tube with t = 5.0 mm, a = 2.0 mm, 2λ = 19.1 mm

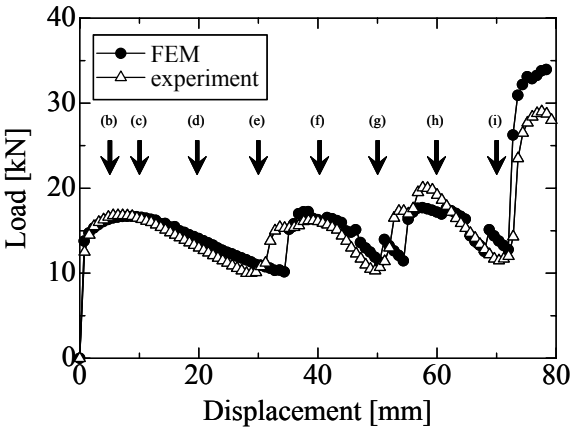

Figure 7 Load-deflection curve of tube with t = 2.0 mm, a = 3.0 mm, 2λ = 30.0 mm

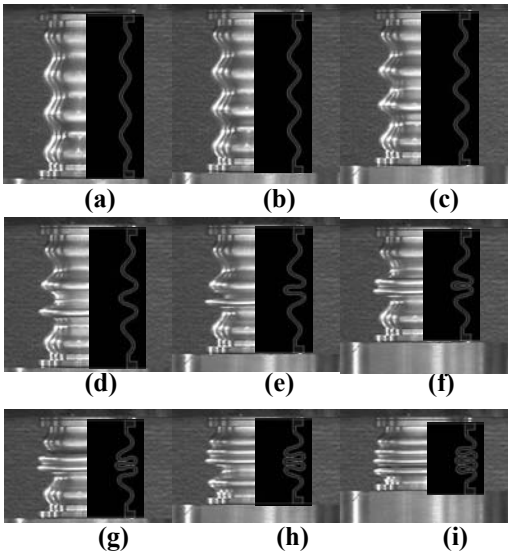

Figure 8 Transformation figures of tube with t = 2.0 mm, a = 3.0 mm, 2λ = 30.0 mm

3.2 Effect of deformation mode produces a dimensional error

The model in which different modes of analysis and experiment, like the P-mode in the experiments and the S-mode in the analysis, is considered to change modes by the slight disturbances in the experiment because it is near the boundary of the P-mode and the S-mode (see Fig.4(b)).

In this study, we investigated the effects of the deformation mode considering a dimensional error of +0.3 to +0.1 in the radius of the part shown in Fig.9 for the analysis model of FEM; *t = 3.0 mm*. Fig.10 shows the mode distribution. It is found from Fig.10 that the geometry, 2λ = 23.3 mm, a = 3.0 mm, 2λ = 19.1 mm, a = 2.0 mm, causes a mode change from the S-mode to the P-mode when the dimensional error is δ = 0.3 [mm]. This geometry is located near the boundary of the S-mode and the P-mode. It is found from Fig.11 that the load–displacement curve obtained experimentally and the dimensional error of 0.3 mm are in good agreement.

Hence, near the boundary of the mode, there is a difference in the deformation mode because of the disturbance due to the dimensional errors. Further, the deformation mode does not change from the P-mode to the S-mode even when there are dimensional errors. Except the case when the mode is different in the experiment and analysis, the load–displacement curve is almost identical. Furthermore, it

can be considered practically permissible because the average load is almost the same in a practical scenario.

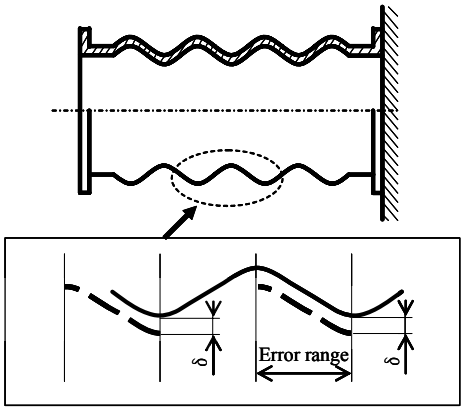

Figure 9 Shape of size error margin model

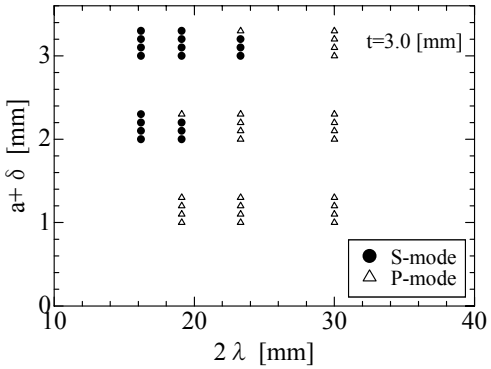

Figure 10 Mode classification chart from size error margin FEM model and experiment

4 Conclusions

In this research, the axial collapse test was performed by using an FEM analysis and an actual specimen on the cylindrical tube with a corrugated surface of an aluminum alloy. The results were as follows:

(1) The reason that a mode did not agree with the analysis and the experiment results was the influence of the initial irregularity. In real materials, the deformation properties are affected by initial imperfections such as dimensional errors. The deformation mode in the analysis and the experiment might change from the S-mode to the P-mode and from the P-mode to the non-symmetric mode. However, there was no change from the P-mode to the S-mode and from the non-symmetric mode to the P-mode.

(2) When the S-mode changed to the P-mode because of the initial imperfections, the load–displacement curve was almost identical. This could be neglected because the average load was almost similar.

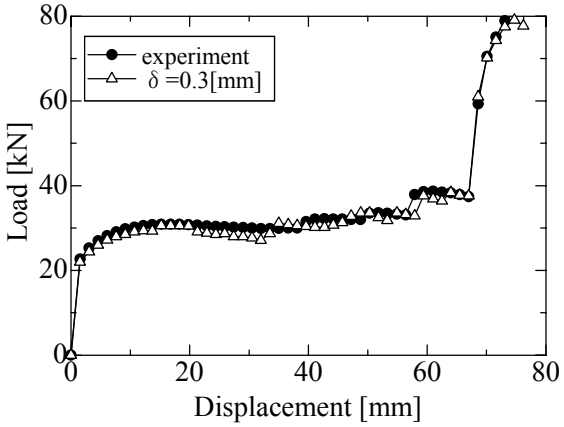

Figure 11 Load–displacement Curve of Tube with t = 3.0 mm, a = 3.0 mm, δ = 0.3 mm, 2λ = 23.3 mm

References

[1] A. A. Singace, H. El-Sobky. Behaviour of Axially Crushed Corrugated Tubes[J]. International Journal of Mechanical Sciences, 1997(39): 249-268

[2] J. F. Carney, R. J. Sazinski. Portable Energy Absorbing System for Highway Service Vehicles[J]. Transportation Engineering Journal, 1987:407-421

[3] B. Skocezen, J. Skizypek. Application of the Equivalent Column Concept to the Stability of Axially Compressed Bellows[J]. International Journal of Mechanical Sciences, 1992(34):901-916

[4] A. M. Elgslsi, E. Mahdi, A. M. S. Hamouda, B. S. Shahari. Crushing Response of Composite Corrugated Tubes to Quasi-Static Axial Loading[J]. Composite Structure, 2004(66): 665-671
[5] T. Hiratsuka, D. Chen and K. Ushijima. Axially Compression of Corrugated Cylinder[J]. The Society of Automotive Engineers of Japan, Paper No.20055304.
[6] D. Chen, T. Hiratsuka. Study of Axially Crushed Cylindrical Tubes with Corrugated Surface Based on Numerical Analysis[J]. Transactions of the Japan Society of Mechanical Engineers, 2006, 72(772): 1464-1471 (In Japanese)
[7] D. Chen, Y. Shimizu. Axially Crushed Square Tubes with Corrugated Surface[J]. Transactions of the Japan Society of Mechanical Engineers, 2006, 72(723):1668-1675 (In Japanese)
[8] D. CHEN, T. Hiratsuka. A Theoretical Analysis of Axially Crushing of Cylindrical Tubes with Corrugated Surface[J]. Transactions of the Japan Society of Mechanical Engineers, 2007, 73(729): 603-610 (In Japanese)
[9] K. Ushijima, S. Haruyama, H. Hanawa, and D. Chen. Strain Concentration for Cylindrical Tubes Subjected to Axial Compression[J]. Transactions of the Japan Society of Mechanical Engineers, 2005, 71(707): 1023-1029 (In Japanese)